Journal of Proteins and Proteomics (2023) 14:81–97
https://doi.org/10.1007/s42485-023-00109-5

RESEARCH

A quantitative proteomic approach revealed variations of salivary proteome during high altitude de-acclimatization

Shikha Jain[1,2] · Swaraj Mohanty[1] · Yasmin Ahmad[1] · Kalpana Bhargava[3]

Received: 6 October 2022 / Revised: 8 December 2022 / Accepted: 29 May 2023 / Published online: 16 June 2023

Abstract

De-acclimatization occurs when an individual returns to sea level after long term exposure to high altitude. Reports on high altitude de-acclimatization document symptoms, physiological changes, and modulations in cardiovascular and nervous systems when individuals descend to sea level. However, there is currently no available data regarding the molecular networks affected by de-acclimatization. The lack of omics-based studies holds necessity of studying molecular signatures and pathways involved in high-altitude de- acclimatization using proteomics-based approach by taking saliva as a diagnostic sample. In this study, we employed iTRAQ based LC-MS/MS approach for comparison between saliva samples obtained from humans ascended from sea level to high altitude and then descended back to sea level followed by pathway analysis using ingenuity pathway analysis (IPA) and validation using immunoassays. Saliva samples were initially taken in normoxic conditions (Baseline 216 m above sea level) with further sampling done at high-altitude exposure (4420 m above sea level) for 30 days (HAD 30) followed by sampling after de- acclimatization (Baseline 216 m above sea level) for 30 days (DI 30). Nearly 152 proteins were found to be differentially expressed in the de-acclimatized group as compared to acclimatized group and normoxia indicating modulated canonical pathways as glycolysis and gluconeogenesis. Carbohydrate metabolism was found to be significantly activated pathway in response to de-acclimatization to high altitude. Collectively, this study provided the initial advancement in understanding high-altitude de-acclimatization mediated events through salivary proteome.

Keywords Saliva · De-acclimatization · High altitude · Proteomics

Abbreviations

iTRAQ	Isobaric tags for relative and absolute quantification
LC–MS/MS	Liquid chromatography based mass spectrometry
ELISA	Enzyme linked immunosorbent assay

✉ Yasmin Ahmad
yasminchem@gmail.com

✉ Kalpana Bhargava
kalpanab2006@gmail.com

[1] Peptide & Proteomics Division, Defence Institute of Physiology & Allied Sciences (DIPAS), Defence R&D Organization (DRDO), Timarpur, New Delhi 110054, India

[2] Present Address: Department of Oral Biology, School of Dental Medicine, University at Buffalo, New York 14214 Buffalo, USA

[3] High Energy Material Research Laboratory (HEMRL), Defence R&D Organization (DRDO), Sutarwadi, Pashan, Pune, Maharashtra 411021, India

Introduction

At high altitude, due to the decreased atmospheric pressure of oxygen, numerous physiological changes need to occur in the body in order to counteract the negative effects of decreased oxygen. These physiological changes can be categorized into short-term changes (acute responses to hypobaric hypoxia) and long-term changes (acclimatization). These long-term changes may be beneficial as opposed to pathological changes and termed as acclimatization. It involves a series of physiological adjustments that compensate for the reduction in ambient PO_2 (Grocott et al. 2007). Protein markers have been studied in rats and humans to understand cellular processes in acclimatized state (Siervo et al. 2014; Luks et al. 2017; Levett et al. 2011; Ahmad et al. 2013; Ahmad et al. 2014; Ahmad et al. 2015; Hartmann et al. 2000; Jain et al. 2020).

Another important condition, High altitude de-acclimatization occurs upon return to sea level after long term exposure to high altitude. As individuals descend to sea level from high altitude, the altitude-acclimatized body suffers

from the stresses induced by re-oxygenation, hyperbaric atmosphere and higher temperatures; and therefore, trigger different pathophysiological signs (Fan et al. 2016). This process involves loss of acclimatization to high altitude over time. In our literature survey, we observed that our previous studies as well as 99.9% studies in the domain of high-altitude hypoxia only talk about high-altitude induction. Only a handful of studies are performed on high-altitude de-acclimatization. Those studies mainly focused on the symptoms; hematological and respiratory parameters; and cardiovascular and nervous system modulations experienced by individuals descended to sea level after exposure to high altitude (Savourey et al. 1996; Boning et al. 1997; Hansen and Sander 2003; Risso et al. 2007; He et al. 2013; Zhao et al. 2016; Mairbaurl 2018; Gonzalez et al. 2005). Some climbers complained of headache, abdominal distention, fatigue, sleepiness and memory loss after descend to sea level from high altitude. A previous omics based study performed on plasma identified a panel of metabolites involved in steroid hormone biosynthesis pathway. This study suggested that those metabolites could be helpful in promoting recovery after injury induced by high altitude-induced hypoxia (Liu et al. 2017). Another omics-based study reported impacts of the plateau environment on the gut microbiota and blood clinical indexes in Han and Tibetan individuals (Jia et al. 2020).

Human saliva being a source of broad spectrum of biomolecules holds promising future among diagnostic samples (Hu et al. 2006; Denny et al. 2008). Recently human salivary proteome have been analyzed by proteomics platforms to characterize 3000 proteins and peptides, most of them are microbiological in origin (Grassl et al. 2016). Besides, approximately 40% of the salivary proteins have been inferred as putative markers for diseases such as cancers mainly oral (Jong et al. 2010; Gallo et al. 2016; Hu et al. 2008), lung (Xiao et al. 2012) and breast cancers (Streckfus et al. 2008); cardiovascular diseases, stroke (Loo et al. 2010); systemic disorders such as hepatitis, HIV, HCV (Hodinka et al. 1998; Yaari et al. 2006); and Sjogren's syndrome (Giusti et al. 2007; Hu et al. 2007; Peluso et al. 2007). Saliva proteome analysis can, therefore, give valuable contributions in understanding pathophysiology of diseases and provide a foundation for the recognition of potential protein markers.

De-acclimatization leads to a number of molecular fingerprints that can be recognized using proteomics analysis. The lack of omics-based studies encouraged the necessity of studying molecular signatures and pathways involved in high-altitude de-acclimatization using proteomics-based approach by taking saliva as a diagnostic sample. The current study explores the informative protein signatures in human salivary proteome along with their potential role in high-altitude de-acclimatization. In this study, we employed iTRAQ based LC–MS/MS approach for comparison between saliva samples obtained from humans ascended from sea level to high altitude and then descended back to sea level followed by pathway analysis using ingenuity pathway analysis (IPA) and validation using immunoassays.

Clinical relevance

Most studies in the domain of high-altitude hypoxia primarily report on high altitude induction, with only a handful of studies focusing on high altitude de-acclimatization. These studies primarily investigate symptoms, hematological and respiratory parameters, and cardiovascular and nervous system modulations experienced by individuals after descending to sea level following high altitude exposure. However, the lack of omics-based studies has highlighted the need to explore molecular signatures and pathways involved in high-altitude de-acclimatization using a proteomics-based approach, utilizing saliva as a diagnostic sample. This present study aims to provide initial advancements in understanding the events mediated by high-altitude de-acclimatization through analyzing the salivary proteome.

Material and methods

All the chemicals unless specified were obtained from Sigma-Aldrich, USA.

Ethical approval and consent to participate

Authorization for all the study protocols was given by institutional ethical committee, Defence Institute of Physiology & Allied Sciences (IEC/DIPAS/B2/1) as per standards set by Declaration of Helsinki and written consent was obtained from all the human volunteers prior to blood collection.

Study groups

Indian male Army troops ($n = 24$, mean age: 30 years; mean weight: 67 ± 0.67 kg) were selected for saliva sampling. Smoking, cardiac disease/defects, hypertension, lung disease/defects, obesity, previous exposure to altitudes 1500 m above sea-level and presence of any infectious/non-infectious disease during cohort study are the exclusion criteria. Samples were initially taken in normoxic conditions (Baseline 216 m above sea level) with further sampling done at high-altitude exposure (4420 m above sea level) for 30 days (HAD 30) followed by sampling after de-acclimatization

(Baseline 216 m above sea level) for 30 days (DI 30). Before sampling, Army troops have gone through the acclimatization protocol as per Indian Army standards (Deshwal et al. 2012). Saliva was collected using passive drooling technique into a pre-chilled falcon followed by centrifugation at 1585×*g* for 15 min at 4 °C to remove insoluble materials, cell debris and other possible contaminants (Jessie et al. 2008; Jain et al. 2018). The protease inhibitor was then added to the supernatant followed by protein estimation using Bicinchoninic Acid (BCA) method (Cat No. BCA1, Sigma-Aldrich, USA) according to manufacturer's protocol. Samples were stored at − 80 °C for further use.

Estimation of oxidative stress parameters

Estimation of reactive oxygen species (ROS)

In saliva, estimation of Reactive Oxygen Species (ROS) levels was performed using a fluorescent dye 2′, 7′-Dichlorofluorescin diacetate (DCFDA) (Cat. No. D6883). In the presence of intracellular reactive oxygen species, the dye enters through cell membrane and cleaves into 2, 7-dichlorofluorescein by the action of intracellular esterase enzymes and produces fluorescence. The generated fluorescence is directly proportional to the reactive oxygen species levels (Wang and Joseph 1999). In brief, 150 µl of undiluted saliva along with 5 µl of 2 mM Dichlorofluorescin diacetate was incubated for 40 min at room temperature in amber tubes in dark. Following incubation, 2 ml of PBS was added to the tubes and 200 µl of each sample was added to 96-well plate (PBS as blank). Fluorescence was measured at excitation and emission wavelengths of 485 nm and 531 nm respectively using an ELISA plate reader (Synergy H1 microplate reader, BioTek USA).

Estimation of lipid peroxidation using thiobarbituric acid reactive substances (TBARS)

Thiobarbituric acid reactive substances (TBARS) assay was performed to estimate lipid peroxidation in saliva. It was measured directly using QuantiChrom™ TBARS Assay Kit (Cat. No. DTBA-100, Bioassays Systems, CA, USA) as suggested by the manufacturer's protocol. In short, standards and samples were prepared by diluting with milli-Q and precipitating with ice-cold 10% TCA, respectively. Following this, TBA was added to the diluted standards and saliva supernatant and incubated at 100 °C for 1 h in water bath. The mixtures were then allowed to cool to RT. Afterwards, 200 µl of the mixtures was poured onto 96-well plate (TBA as blank) and the absorbance was measured at 535 nm using spectrophotometer (EON Biotech, USA).

Estimation of activity of antioxidant enzymes

Estimation of catalase activity

In saliva, activity of catalase enzyme was estimated using EnzyChromTM Catalase Assay Kit (Cat No. ECAT-100, Bioassay systems, USA) according to manufacturer's instructions. In brief, 4.8 mM H2O2 was used to prepare standards. 10 µl of the standards or samples along with 90 µl of 50 µM H2O2 substrate were added onto the microplate and incubated for 30 min at RT. Further, plate was incubated with 100 µl of detection reagent for 10 min at RT and the absorbance was recorded at 570 nm using microplate reader (EON Biotech, USA).

Estimation of reduced glutathione

Reduced glutathione levels were estimated in human saliva samples using microplate assay kit (Cat. No. CS0260) as per manufacturer's instructions. Briefly, standards were reconstituted and serially diluted with milli-Q and 5% 5-sulfosalicylic acid (SSA), respectively. Standards and samples were mixed with working mixture (assay buffer, enzyme and 5, 5-dithiobis-2-nitrobenzoic acid (DTNB) solution) and incubated for 5 min at RT followed by addition of NADPH solution to each well. End-point absorbance was recorded after 5 min of incubation at 412 nm using a microplate reader (EON Biotech, USA).

Sodium dodecyl-sulfate polyacrylamide gel electrophoresis (SDS-PAGE)

The samples were prepared for 12% SDS-PAGE by mixing with 5× sample buffer followed by boiling at 100 ºC for 10 min and kept at − 20 ºC for 5 min. Meanwhile, 12% resolving and 5% stacking gels were prepared and poured between the plates and allowed to set for 20–30 min. The samples (~ 20 µg of protein/well) were loaded into the wells and gel was run on electrophoresis system (GE Healthcare) at 10 mA/gel and 20 mA/gel in stacking and resolving gel, respectively.

Staining and imaging

Protein bands were visualized using modified silver staining procedure compatible with mass spectrometry (Yan et al. 2000). In brief, procedure included the following six steps: (a) fixation using fixing solution for 2 h to overnight, (b) washing with washing solution for 20 min, (c) sensitization

with sensitizing solution followed by two washings with Milli-Q water each for 1 min, (d) staining in silver nitrate solution for 20 min followed by rinse with Milli-Q water for 1 min, (e) development of spots using developing solution and (f) termination of reaction by adding stopping solution.

The SDS-PAGE gel images stained with silver nitrate were digitalized using ChemiDoc™ XRS + imaging system (Cat No. 1708265, Bio-Rad Laboratories).

High throughput proteomics using LC–MS/MS

Sample preparation

100 µg of protein from saliva samples was dispensed in 30 µl of dissolution buffer and processed for LC–MS/MS using iTRAQ kit (Cat No. 4352135, ABSciex, USA). Processing includes the following three steps: (a) denaturation using 1 µl of denaturant, (b) reduction by incubation with 2 µl of reducing agent at 60^0C for 1 h and (c) alkylation using 1 µl of cysteine blocking agent followed by overnight in-solution trypsin digestion using trypsin singles proteomics grade (Cat no. T7575). The digested peptides were then labeled with iTRAQ reagents (activated with isopropanol) and incubated for 2 h at RT. SCX cartridge (5 micron, 300 Å bead from ABSciex, USA) was used to fractionate samples into fractions eluted at 35 mM, 50 mM, 75 mM, 100 mM, 125 mM, 150 mM, 250 mM, 350 mM, 500 mM ammonium formate buffer (ammonium formate, 30% v/v Acetonitrile (ACN) and 0.1% formic acid; pH = 2.9) and got analyzed individually on quadrupole-TOF hybrid mass (Triple TOF 5600 & 6600, Sciex USA) spectrometer coupled to an EksigentNanoLC-Ultra 2D plus system.

Mass spectrometry (LC–MS/MS)

Each sample fraction was poured onto a trap column (200 µm × 0.5 mm) and desalted at flow rate of 2 µL/min for 45 min followed by peptide separation using a nano-C18 column (75 µm × 15 cm) through a gradient method with buffer A (99.9% LC–MS water + 0.1% formic acid) and buffer B (99.9% acetonitrile + 0.1% formic Acid). Data was obtained in an information-dependent acquisition mode with MS settings as follows: nebulizing gas of 25; a curtain gas of 25; an Ion spray voltage of 2400 V and heater interface temperature of 130 °C followed by TOFMS scan in the mass range of 400–1600 m/z with accumulation time of 250 ms and, the MS/MS product ion scan in the mass range of 100–1800 m/z for 70 ms with a total cycle time of 2.05 s approximately. Parent ions with abundance > 150 cps and with a charge state of + 2 to + 5 were selected for MS/MS fragmentation followed by exclusion of its mass and isotopes for 3 s. Further, MS/MS spectra were obtained with adjust collision energy setting with high-sensitivity mode when using iTRAQ reagent. Raw data files were searched against the most recent database for Human downloaded from UniProt using the MudPIT option in Proteome Discoverer 2.2 (Thermo Scientific) and the Sequest HT search algorithm. For protein identification results, only peptides identified with high confidence were used. For confidence, the Percolator algorithm was used for PSM (peptide spectrum match) validation in database searches. The False Discovery Rate (FDR) threshold calculated in Proteome Discoverer Percolator when high confidence peptides was used for protein identification is 0.01. Abundance Ratios > 1.5 were classified as up-regulated, < 0.67 were classified as down-regulated. Ratios from 1.5 to 0.67 were considered moderate to no changes.

Pathway analysis of proteomics data

Results obtained from high-throughput LC–MS/MS were sorted based on FDR < 1 (false discovery rate) and p value < 0.05. Selected proteins with their respective abundance ratios were analyzed using network analysis tool, Ingenuity Pathway analysis (IPA, Qiagen) with inbuilt statistical analysis package. Fold change ≥ 1.5 was set as cutoff for various programs such as canonical pathways, disease networks and functions and proteins networks. These networks played essential role in suggesting key changes in the cellular events, biochemical processes and molecular cascades. To predict the directionality of the cellular event, a significant positive and negative z score was used. Top canonical pathways and molecular events were selected using minimum p value criteria.

Immunoassays (ELISA)

ELISA assay was performed ($n = 24$ in each group) for Alpha-enolase (Cat No. ab181417, Abcam, Cambridge, UK) as per the respective manufacturer's protocol.

Immunoblotting

After SDS-PAGE, gels were transferred onto 0.45 µm nitrocellulose membrane (Cat No. 1620115, Bio-Rad Laboratories) using semi-dry power blotter XL System (Cat No. PB0013, ThermoFisher Scientific). The membrane was carefully blocked in the blocking buffer containing 5% Skim Milk (Cat No. GRM1254, HiMedia) dissolved in Phosphate Buffer Saline (PBS) [pH-7.4] containing 0.1% Tween-20(PBST) for 2 h at room temperature. Then, the membrane was incubated with Trx antibody (Cat No. ab16965, Abcam)

[1:2000 dilution] at 4 °C overnight. Subsequently, the membrane was washed thrice with 0.1% PBST for 10 min each on an orbital shaker followed by incubation with secondary antibody anti-mouse IgG (Cat No. A9044, Sigma Life Science) [1:20,000 dilution] for 2 h at room temperature. The membrane was finally washed thrice for 10 min each with 0.1% PBST solution. The blot was developed on Chemi-DocTM XRS + imaging system (Cat No. 1708265, Bio-Rad Laboratories), using Chemiluminescent Peroxidise Substrate (Cat No. CPS1120-1KT, Sigma).

The images were analysed with Image J software (https://imagej.nih.gov/ij/) for the pixel densitometry.

Statistical analysis

Graphpad Prism (Version 9) was used for statistical analysis of immunoblots and assays and p values were calculated based on repeated measures one-way ANOVA with Tukey's multiple comparison test with $p < 0.05$ as cut-off for significance. Mean (95% confidence interval) values were used for preparing the graphs.

Results

Modulations in oxidative stress parameters and antioxidant enzymes after de-acclimatization from high altitude to sea level

Hypobaric hypoxia mainly modulates oxidative stress parameters; therefore the levels of oxidative stress parameters were analysed using saliva samples. The levels of reactive oxygen species (ROS) and lipid peroxidation [using Thiobarbituric acid reactive substances (TBARS)] were measured.

ROS levels were found to be increased at HAD 30 group as compared to N (p value: 0.090) followed by a significant decrease at DI 30 as compared to HAD 30 group (p value: 0.029). The levels of ROS at DI 30 group were found to be normalized as compared to N (p value: 0.707) (Fig. 1a). The TBARS levels corresponding to lipid peroxidation showed non-significant minimal modulation in DI 30 group when compared to N or HAD 30 group (p value: 0.569) (Fig. 1b).

Antioxidants are responsible for providing protection to the damage caused by oxidative stress; therefore, activity of antioxidants such as activity of catalase and reduced glutathione was estimated.

Catalase activity showed no difference at HAD 30 group as compared to N and at DI 30 group as compared to HAD30 (p value: 0.132) (Fig. 2a). The levels of reduced glutathione were observed to be normalized in DI 30 group as compared to N or HAD 30 (p value: 0.919) (Fig. 2b).

Human salivary proteome analysis using LC–MS/MS based quantification

We initiated our investigation by analyzing the salivary proteome of individuals who traveled from high altitude to sea level (DI 30 group) using iTRAQ labeling and LC-MS/MS analysis. This group was compared with the HAD 30 group and normoxic controls. An enormous number of proteins has been perceived in saliva to understand the casual events occurring after travel from high altitude to sea level. In total 380 proteins were identified and mentioned in

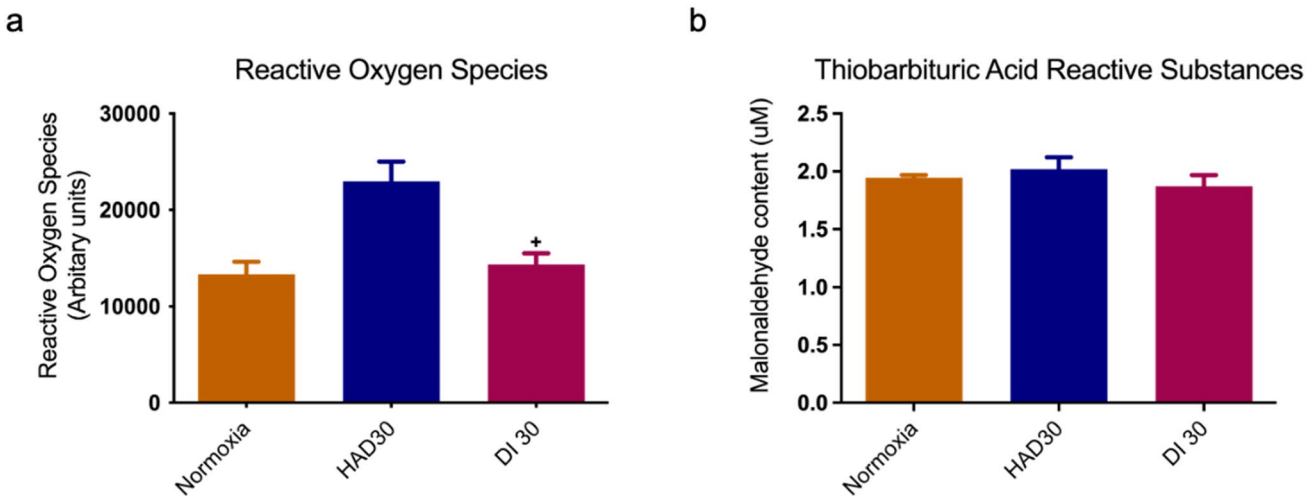

Fig. 1 Modulations in oxidative stress parameters **a** Levels of reactive oxygen species were measured showing an increased levels of ROS at HAD30 group as compared to N followed by decreased levels at DI 30 group as compared to HAD30. **b** TBARS levels were measured and found to be normalized in every group. Results are expressed as Mean concentration ± SD. Mean was calculated from three separate experiments ($^{+}$represents $p < 0.05$ with respect to HAD30, sample size = 24)

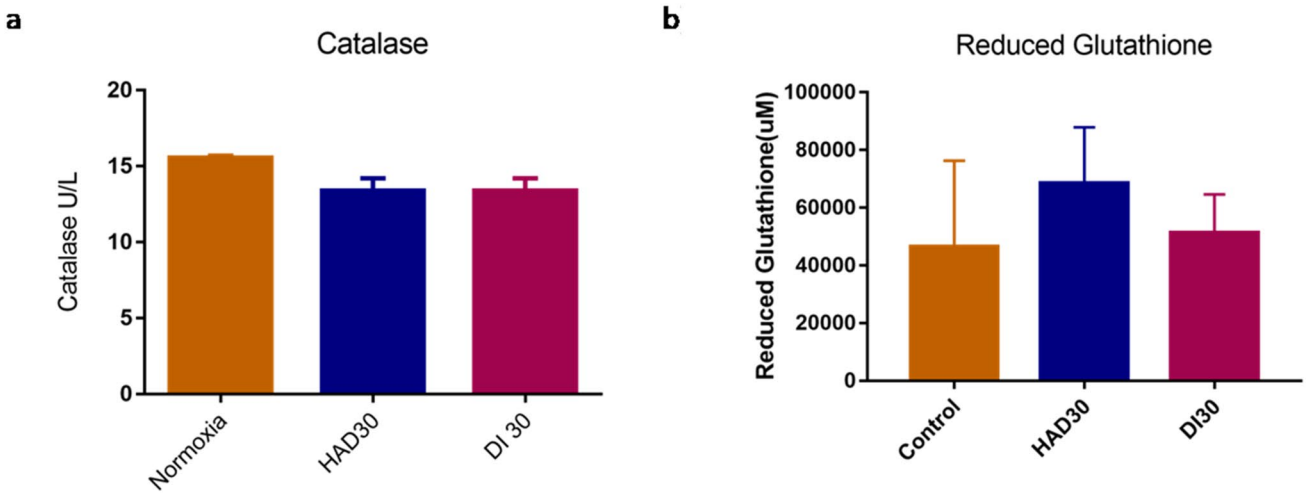

Fig. 2 Antioxidant status **a** Catalase activity showed no significant difference in the levels of catalase activity at HAD30 group as compared to N and at DI 30 group as compared to HAD30. **b** Levels of reduced glutathione were measured and observed to be normalized in DI 30 group as compared to N or HAD30. Results are expressed as Mean concentration ± SD. Mean was calculated from three separate experiments (sample size = 24)

supplementary material (Table S1), out of which 152 proteins were differentially expressed in DI 30 group as compared to normoxia and HAD 30 group (Table 1).

Out of three hundred and eighty proteins, 98 proteins were differentially expressed in DI 30 group as compared to normoxic controls in which 32 proteins were up-regulated and 66 proteins were down-regulated. In DI 30 as compared to HAD 30, 95 proteins were found to be differentially expressed out of which 63 and 32 proteins were up-regulated and down-regulated respectively (Fig. 3a).

Forty-one proteins were commonly observed in DI 30 as compared to normoxic controls and HAD 30 group. Venn diagram depicts the common number of proteins between de-acclimatization group when compared to high-altitude induction group and normoxic controls (Fig. 3b). Pathway analysis through IPA software revealed pathways such as LXR/RXR activation, acute-phase response signaling, glycolysis and gluconeogenesis to be the most significant pathways in DI 30/N and DI 30/HAD 30 (Fig. 3c). LXR/RXR activation and acute phase response signaling pathway were down-regulated (z score < -1); and Glycolysis and Gluconeogenesis were up-regulated (z score > 1).

LXR/RXR activation and acute phase response signaling pathways were also found to be significant in HAD30 as compared to N (Supplementary Material, Fig. S5). Key proteins found to be modified in LXR/RXR activation were Apolipoprotein A-I (ApoA1), Interleukin 1 (IL36RA), Alpha-1-antitrypsin (SERPINA1), Transthyretin (TTR), Complement C4-A (C4A), Monocyte differentiation antigen CD14, Phospholipid transfer protein (PLTP), Kininogen 1, Alpha-2-HS-glycoprotein (AHSG), ITIH4 protein, Apolipoprotein B (ApoB), Apolipoprotein D (ApoD), Vitronectin (VTN), Fibrinogen alpha chain (FGA), Beta-2-glycoprotein 1 (ApoH), Alpha-1-acid glycoprotein 1 (ORM1), Serum albumin, Vitamin D-binding protein (GC), Hemopexin (HPX), Protein S100-A8, Clusterin, Matrix metalloproteinase-9 (MMP9), Interleukin-1 receptor antagonist protein (IL1RA), Alpha-1-acid glycoprotein 2 (ORM2), Lysozyme C (LYZ), Transferrin, Interleukin-36 alpha (IL36A), Complement C3 and Alpha-1B-glycoprotein (A1BG) (Supplementary Material, Fig. S6).

Another pathway, acute phase response signaling is a major contributor to oxidative stress induced by high altitude. Key proteins observed to be modulated in this pathway were Apolipoprotein A-I (ApoA1), Fibronectin 1 (FN1), Interleukin 1 (IL36RA), Alpha-1-antitrypsin (SERPINA1), Transthyretin (TTR), Complement C4-A (C4A), ceruloplasmin (CP), histidine-rich glycoprotein (HRG), Alpha-1-antichymotrypsin (SERPINA3), Alpha-2-HS-glycoprotein (AHSG), ITIH4 protein, Fibrinogen gamma chain (FGG), Haptoglobin (HP), Alpha-2-macroglobulin (A2M), Fibrinogen alpha chain (FGA), Beta-2-glycoprotein 1 (ApoH), Alpha-1-acid glycoprotein 1 (ORM1), Serum albumin, Hemopexin (HPX), Interleukin-1 receptor antagonist protein (IL1RA), Alpha-1-acid glycoprotein 2 (ORM2), Cellular retinoic acid-binding protein 2 (CRABP2), Transferrin, Interleukin-36 alpha (IL36A),

Table 1 Overview of human salivary proteins differentially expressed in DI 30 group with respect to normoxic control and HAD 30 group along with their Uniprot IDs and abundance ratios

S. no.	Name of the protein	Gene ID	Uniprot ID	Abundance ratio (DI 30/N)	Abundance ratio (DI 30/HAD 30)
1	Serum albumin	ALB	P02768	0.495	0.97
2	Alpha-amylase 1	AMY1A	P04745	0.956	0.485
3	Mucin 5AC, oligomeric mucus/gel-forming	MUC5AC	A7Y9J9	0.444	0.641
4	Lactoferrin	LTF	B3VMW0	0.693	0.474
5	Lactoferrin	LTF	W8QEY1	0.745	0.554
6	Actin, cytoplasmic 2	ACTG1	P63261	1.439	1.662
7	Epididymis secretory sperm binding protein Li 62p	HEL-S-62p	V9HWA9	0.637	0.844
8	Alpha-2-macroglobulin-like protein 1	A2ML1	A8K2U0	1.448	1.769
9	cDNA FLJ78096, highly similar to Homo sapiens actin, alpha, cardiac muscle (ACTC), mRNA		A8K3K1	1.804	2.352
10	Cystatin-S OS = Homo sapiens	CST4	P01036	1.978	1.502
11	Immunoglobulin alpha-2 heavy chain		P0DOX2	1.663	1.24
12	Alpha-enolase	ENO1	P06733	1.295	1.833
13	HCG2039812, isoform CRA_b (Fragment)	KRT6A	A0A0S2Z428	2.003	2.056
14	IGH@ protein	IGH@	Q6GMX6	0.657	0.956
15	Cystatin-SA	CST2	P09228	2.084	1.557
16	Prolactin-inducible protein	PIP	P12273	1.873	1.388
17	Epididymis luminal protein 57	HEL57	V9HWH1	1.293	1.591
18	cDNA FLJ60163, highly similar to Carbonic anhydrase 6 (EC 4.2.1.1)		B4DUH8	0.887	0.498
19	IGL@ protein	IGL@	Q6PIK1	1.559	1.093
20	Uncharacterized protein DKFZp686I04196 (Fragment)	DKFZp686I04196	Q6N093	0.5	0.922
21	Heat shock 70 kDa protein 1A variant (Fragment)		Q59EJ3	1.26	1.553
22	Alpha-1-antitrypsin	SERPINA1	A0A024R6I7	0.555	0.92
23	Zymogen granule protein 16 homolog B	ZG16B	Q96DA0	1.157	0.551
24	Epididymis luminal protein 33	HEL-S-72p	V9HW22	1.254	1.973
25	cDNA FLJ78643, highly similar to Homo sapiens cornulin (CRNN), mRNA		A8K5I6	1.93	1.596
26	Glyceraldehyde-3-phosphate dehydrogenase	GAPDH	P04406	1.953	1.947
27	Haptoglobin	HP	H0Y300	0.601	0.993
28	Lipocalin-1	LCN1	P31025	0.213	0.442
29	Immunoglobulin heavy constant gamma 4	IGHG4	P01861	0.5	0.899
30	Protein S100-A9	S100A9	P06702	1.156	2.226
31	14-3-3 protein zeta/delta	YWHAZ	P63104	1.434	2.159
32	Beta-globin	HBB	D9YZU5	0.329	1.126
33	Protein-glutamine gamma-glutamyltransferase E	TGM3	Q08188	1.429	1.904
34	6-phosphogluconate dehydrogenase, decarboxylating	PGD	P52209	1.367	1.567
35	Isoform H7 of Myeloperoxidase	MPO	P05164-3	0.504	0.868
36	CSTB protein	CSTB	Q76LA1	1.501	2.506
37	Isoform 3 of Interleukin-1 receptor antagonist protein	IL1RN	P18510-3	1.889	2.345
38	Annexin A1	ANXA1	P04083	2.704	2.482
39	Cystatin-A	CSTA	P01040	1.068	1.551
40	cDNA, FLJ93674		B2R7Z6	0.361	0.569
41	Epididymis secretory protein Li 22	HEL-S-22	V9HWE9	1.26	1.549
42	Epididymis secretory sperm binding protein Li 78p	HEL-S-78p	V9HVY1	0.649	0.868
43	Thioredoxin	TXN	H9ZYJ2	1.772	2.457
44	Histone H4	HIST1H4A	P62805	0.606	1.075
45	IgG H chain		S6BGE0	0.449	0.597

Table 1 (continued)

S. no.	Name of the protein	Gene ID	Uniprot ID	Abundance ratio (DI 30/N)	Abundance ratio (DI 30/HAD 30)
46	Catalase	CAT	P04040	0.655	0.992
47	cDNA FLJ76826, highly similar to Homo sapiens ceruloplasmin (ferroxidase) (CP), mRNA		A8K5A4	0.611	0.823
48	Calmodulin-like protein 3	CALML3	P27482	1.274	1.647
49	Epididymis secretory protein Li 102	HEL-S-102	V9HW43	1.966	1.91
50	Alpha-1-acid glycoprotein 1	ORM1	P02763	0.656	1.004
51	Peptidyl-prolylcis-trans isomerase		A8K486	1.463	1.791
52	Globin C1	GLNC1	A0A1K0GXZ1	0.374	0.992
53	Hemopexin	HPX	P02790	0.503	0.92
54	Epididymis secretory protein Li 34	PEBP1	D9IAI1	1.273	1.512
55	Cystatin-D	CST5	P28325	1.538	1.212
56	Isoform 3 of L-lactate dehydrogenase A chain	LDHA	P00338-3	1.503	1.397
57	Serpin B13	SERPINB13	A0A0A0MQW3	1.373	1.971
58	SCCA2/SCCA1 fusion protein isoform 1		Q5K634	0.996	0.532
59	ALDH3A1 protein (Fragment)	ALDH3A1	Q6PKA6	1.73	1.576
60	Apolipoprotein A-I, isoform CRA_a	APOA1	A0A024R3E3	0.423	0.884
61	Basic salivary proline-rich protein 2	PRB2	P02812	4.101	0.086
62	Matrix metalloproteinase-9	MMP9	P14780	0.966	1.67
63	Protein S100-A8	S100A8	P05109	1.279	1.719
64	Histone H2B		B4DR52	0.562	1.026
65	Serpin peptidase inhibitor, clade C (Antithrombin), member 1, isoform CRA_a	SERPINC1	A0A024R944	0.577	0.771
66	Alpha-1-acid glycoprotein 2	ORM2	P19652	0.6	0.717
67	Isoform 3 of Vitamin D-binding protein	GC	P02774-3	0.644	0.869
68	Isoform 4 of Alpha-actinin-1	ACTN1	P12814-4	0.651	1.456
69	Small proline-rich protein 3	SPRR3	Q9UBC9	2.606	3.023
70	Fibrinogen alpha chain	FGA	P02671	0.609	0.952
71	Mucin-7	MUC7	Q8TAX7	0.877	0.653
72	Collagen alpha-1 (VI) chain	COL6A1	P12109	0.74	0.564
73	Epididymis secretory sperm binding protein Li 2a	HEL-S-2a	V9HW12	1.198	1.569
74	Antileukoproteinase	SLPI	P03973	0.872	0.565
75	Monocyte differentiation antigen CD14		B2R888	0.963	0.469
76	cDNA, FLJ92164, highly similar to Homo sapiens peroxiredoxin 1 (PRDX1), mRNA		B2R4P2	1.308	1.539
77	F-box only protein 50	NCCRP1	Q6ZVX7	1.768	2.102
78	Glycogen phosphorylase, liver form	PYGL	P06737	0.881	1.609
79	Myeloblastin	PRTN3	P24158	0.474	1.472
80	Rab GDP dissociation inhibitor		B4DLV7	1.037	2.422
81	Carboxylic ester hydrolase	CES2	A0A024R6X1	1.049	1.622
82	Submaxillary gland androgen-regulated protein 3B	SMR3B	P02814	4.797	0.928
83	IBM-B2 heavy chain variable region (Fragment)		A0A125QYY9	1.243	1.607
84	Azurocidin	AZU1	P20160	0.569	0.862
85	Kininogen 1, isoform CRA_b	KNG1	B4E1C2	0.555	0.683
86	HEBP2 protein (Fragment)	HEBP2	Q05DB4	1.31	0.608
87	Isoform 2 of Nucleoside diphosphate kinase A	NME1	P15531-2	1.322	1.746
88	Transthyretin	TTR	A0A087WT59	0.511	0.838
89	Histone H3		A8K4Y7	0.408	1.027
90	Histone H2A	HIST1H3D	A0A0U1RRH7	0.495	0.917
91	ITIH4 protein	ITIH4	B7ZKJ8	0.638	0.798

Table 1 (continued)

S. no.	Name of the protein	Gene ID	Uniprot ID	Abundance ratio (DI 30/N)	Abundance ratio (DI 30/HAD 30)
92	Sulfhydryl oxidase 1	QSOX1	O00391	0.713	0.544
93	Fibronectin 1, isoform CRA_n	FN1	A0A024R462	0.58	0.796
94	Hypoxia up-regulated protein 1	HYOU1	Q9Y4L1	0.643	0.627
95	HRV Fab 027-VL (Fragment)		A2IPI6	0.24	0.669
96	Phosphoglucomutase-2	PGM2	Q96G03	1.553	1.957
97	Galectin (Fragment)		Q59FR8	0.633	1.067
98	cDNA FLJ75422, highly similar to Homo sapiens capping protein (actin filament) muscle Z-line, alpha 1, mRNA		A8K0T9	0.968	1.53
99	Neutrophil defensin 1	DEFA1	P59665	0.583	1.476
100	Galectin-10	CLC	Q05315	0.583	1.226
101	Protein S100-P	S100P	P25815	0.581	1.051
102	SH3 domain binding glutamic acid-rich protein like 3, isoform CRA_a (Fragment)	SH3BGRL3	D3DPK5	0.494	0.906
103	Furin	FURIN	P09958	0.564	0.627
104	Ig heavy chain variable region (Fragment)		A0A068LKQ8	1.124	1.526
105	ARP3 actin-related protein 3 homolog (Yeast), isoform CRA_a	ACTR3	A0A024RAI1	0.531	0.84
106	cDNA, FLJ93914, highly similar to Homo sapiens histidine-rich glycoprotein (HRG), mRNA		B2R8I2	1.208	0.451
107	MS-C3 light chain variable region (Fragment)		A0A125U0U8	0.629	0.815
108	Superoxide dismutase [Cu–Zn]	HEL-S-44	V9HWC9	1.256	1.524
109	cDNA, FLJ93654, highly similar to Homo sapiens serpin peptidase inhibitor, clade B (ovalbumin), member 2 (SERPINB2), mRNA		B2R7Y0	1.533	1.783
110	Apolipoprotein D (Fragment)	APOD	C9JF17	0.58	1.064
111	Small proline rich protein		Q2I377	1.322	1.718
112	Basic salivary proline-rich protein 3	PRB3	F5H7C1	1.956	0.249
113	Epididymis luminal protein 114	HEL114	V9HWK2	0.638	0.963
114	cDNA FLJ50663, highly similar to Phosphoglucomutase-1 (EC 5.4.2.2)		B7Z6C2	0.529	0.742
115	Aspartate aminotransferases	GOT2	A0A024R6W0	0.448	0.983
116	Rheumatoid factor RF-IP24 (Fragment)		A2J1N4	0.624	0.722
117	Proline-rich protein 4	PRR4	A0A087WY73	2.607	2.807
118	Interleukin-36 alpha	IL36A	Q9UHA7	1.392	1.546
119	Rho GDP-dissociation inhibitor 1	ARHGDIA	J3QQX2	1.082	2.43
120	Neutrophil elastase	ELANE	P08246	0.485	1.578
121	Aminopeptidase B	RNPEP	Q7RU04	0.582	1.758
122	Histone H1.5	HIST1H1B	P16401	0.7	0.658
123	Epididymis luminal protein 220	HEL-S-70	V9HW80	0.305	2.047
124	Glutamine synthetase	GLUL	P15104	1.667	1.903
125	E3 ubiquitin-protein ligase TRIM56	TRIM56	Q9BRZ2	0.432	0.73
126	Aquaporin-5	AQP5	P55064	0.421	0.662
127	Beta-2-glycoprotein 1	APOH	P02749	0.478	0.578
128	Leukotriene B4 12-hydroxydehydrogenase, isoform CRA_a	LTB4DH	A0A024R172	1.114	1.888
129	Uncharacterized protein		B7ZLF8	1.515	2.165
130	cDNA, FLJ93711, highly similar to Homo sapiens myeloid cell nuclear differentiation antigen (MNDA), mRNA		B2R829	0.607	0.66
131	Macrophage migration inhibitory factor	MIF	P14174	1.666	3.065
132	Protein S100-A7	S100A7	P31151	0.542	1.342
133	Vitamin D binding protein (Fragment)	GC	A0A1B1CYC5	0.554	0.504

Table 1 (continued)

S. no.	Name of the protein	Gene ID	Uniprot ID	Abundance ratio (DI 30/N)	Abundance ratio (DI 30/HAD 30)
134	Bactericidal permeability-increasing protein	BPI	P17213	0.566	0.785
135	Mannosyl-oligosaccharide 1,2-alpha-mannosidase IA	MAN1A1	P33908	0.516	0.555
136	Interleukin 1 family, member 5 (Delta), isoform CRA_a	IL1F5	A0A024R518	0.71	0.57
137	Isoform A of protein FAM3B	FAM3B	P58499-2	0.657	0.563
138	Isoform 3 of complement C1q tumor necrosis factor-related protein 3	C1QTNF3	Q9BXJ4-3	0.981	0.457
139	BJ-HCC-24 tumor antigen		Q9NXW1	1.488	2.507
140	Peroxiredoxin-5, mitochondrial	PRDX5	P30044	1.565	1.699
141	Immunoglobulin lambda variable 2–11	IGLV2-11	P01706	1.599	1.224
142	Epididymis secretory sperm binding protein Li 128 m	HEL-S-128 m	V9HWC7	1.165	1.82
143	D-dopachrome decarboxylase	DDT	J3KQ18	0.751	2.094
144	Glucosidase, alpha acid (Pompe disease, glycogen storage disease type II), isoform CRA_a	GAA	A0A024R8Q1	0.504	0.736
145	Apolipoprotein B (Including Ag(X) antigen)	APOB	C0JYY2	0.442	0.673
146	Thioredoxin domain-containing protein 17	TXNDC17	Q9BRA2	0.992	1.838
147	Protein S100		B2R577	0.923	1.608
148	Acid ceramidase (Fragment)	ASAH1	A0A1B0GVC9	2.184	1.472
149	cDNA FLJ57644, highly similar to Serum paraoxonase/arylesterase 1 (EC 3.1.1.2)		B4DX19	0.488	0.757
150	Cellular retinoic acid-binding protein 2	CRABP2	P29373	1.647	1.613
151	Cathepsin G	CTSG	P08311	0.34	0.465
152	Nuclear transport factor 2	NUTF2	P61970	0.76	1.793

Fibrinogen beta chain (FGB) and Complement C3 (Supplementary Material, Fig. S7).

De-acclimatization to hypobaric hypoxia activates carbohydrate metabolism

Carbohydrate metabolism, mainly glycolysis and gluconeogenesis, pathways were found to be activated on de-acclimatization to sea level as compared to high-altitude exposure group (DI 30/HAD 30) and sea level normoxic controls (DI 30/N). An expanded view of IPA mined glycolysis and gluconeogenesis pathway is shown with overlaid modulated proteins (pink outlined) identified in saliva proteome (Fig. 4). Key proteins modulated in this pathway were Glucose-6-phosphate isomerase, Fructose-bisphosphate aldolase, Phosphoglycerate kinase 1, Fructose-bisphosphate aldolase A, Glyceraldehyde-3-phosphate dehydrogenase, Alpha-enolase, Triosephosphate isomerase, Phosphoglycerate mutase, Pyruvate kinase, Malate dehydrogenase 2 and Malate dehydrogenase 1 (Fig. 5a). Out of these proteins, alpha-enolase levels were up-regulated (nearly twofolds) in DI 30 group as compared to HAD30. Therefore, it was validated in saliva samples of N, HAD30 and DI 30 groups using ELISA. The levels decreased in HAD30 from N (p value: 0.039) followed by an increase in DI 30 group as compared to HAD30 (p value: 0.039) (Fig. 5b).

An unrelated redox protein, thioredoxin (Trx) was found to be up-regulated (nearly fourfolds) in DI 30 group as compared to HAD30. Therefore, it was also validated in saliva samples of N, HAD30 and DI 30 groups using immunoblotting. The levels decreased in HAD30 from N (p value: 0.032) followed by an increase in DI 30 group as compared to HAD30 (p value: 0.042) (Fig. 6).

Discussion

De-acclimatization is a process involving loss of acclimatization to high altitude over time. A handful of earlier studies on high-altitude de-acclimatization mainly focused on the following symptoms: hematological and respiratory parameters and cardiovascular and nervous system modulations experienced by individuals descended to sea level after exposure to high altitude. Some climbers complained

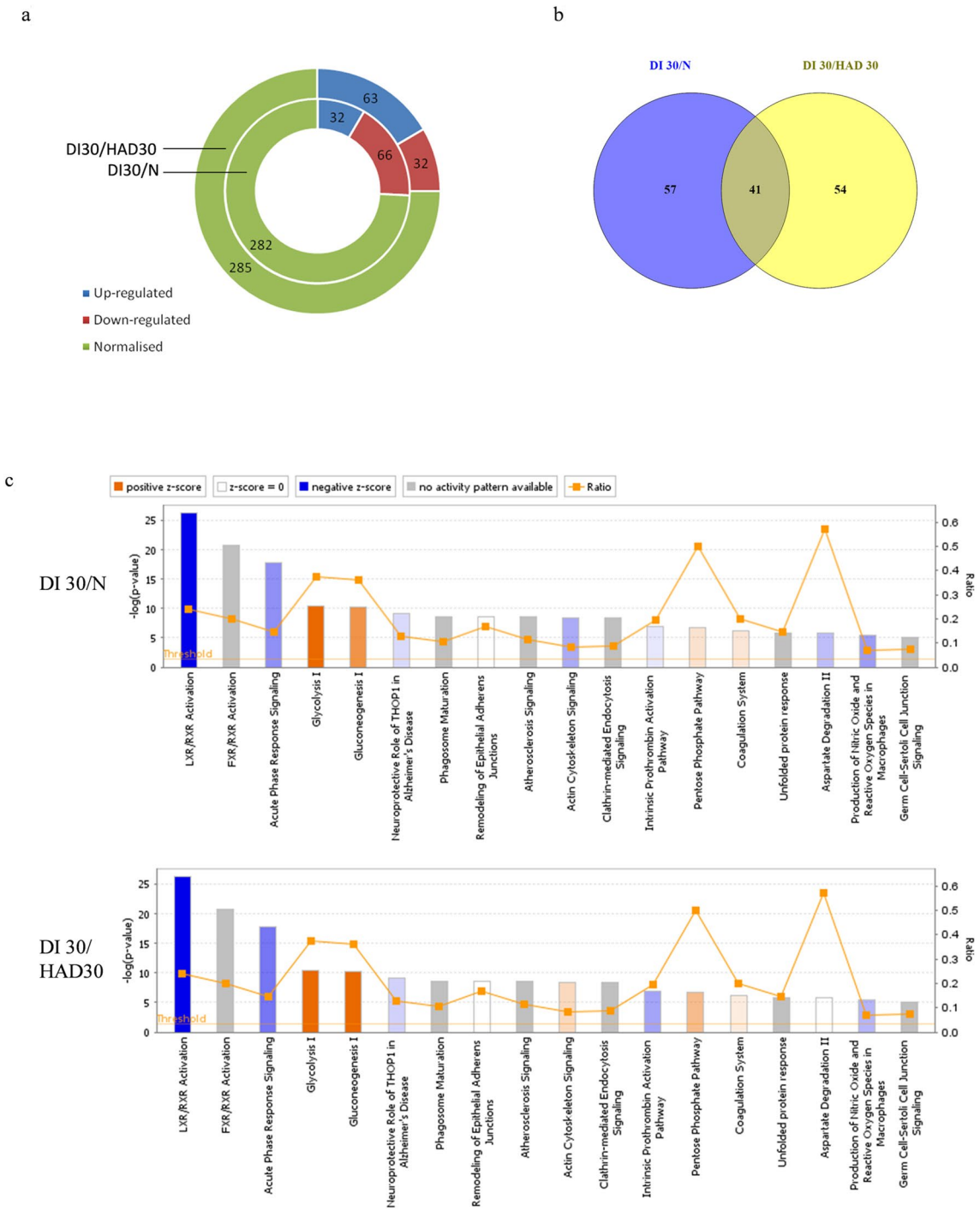

Fig. 3 Overview of human salivary proteome during de-induction from high altitude to sea level along with affected pathways. **a** The total number of up-regulated (red) and down-regulated (green) proteins along with normalized proteins (blue) identified through LCMS/MS (iTRAQ labeled) analysis of human saliva in DI30 group as compared to HAD30 and normoxia. Abundance ratios ≥ 1.5 and ≤ 0.67 were considered as up-regulation and down-regulation respectively. **b** Venn diagram of overlapping number of differentially modulated proteins among DI30/N (blue) and DI30/HAD30 (yellow) groups using Oliveros, J.C. (2007–2015) Venny. An interactive tool for comparing lists with Venn's diagrams. http://bioinfogp.cnb.csic.es/tools/venny/index.html. **c** IPA revealed presence of pathways such as LXR/RXR activation, acute phase response signaling, glycolysis, gluconeogenesis and pentose phosphate pathway to be the most significant pathways in DI30/N and DI30/HAD30 based on p value < 0.001 and z score

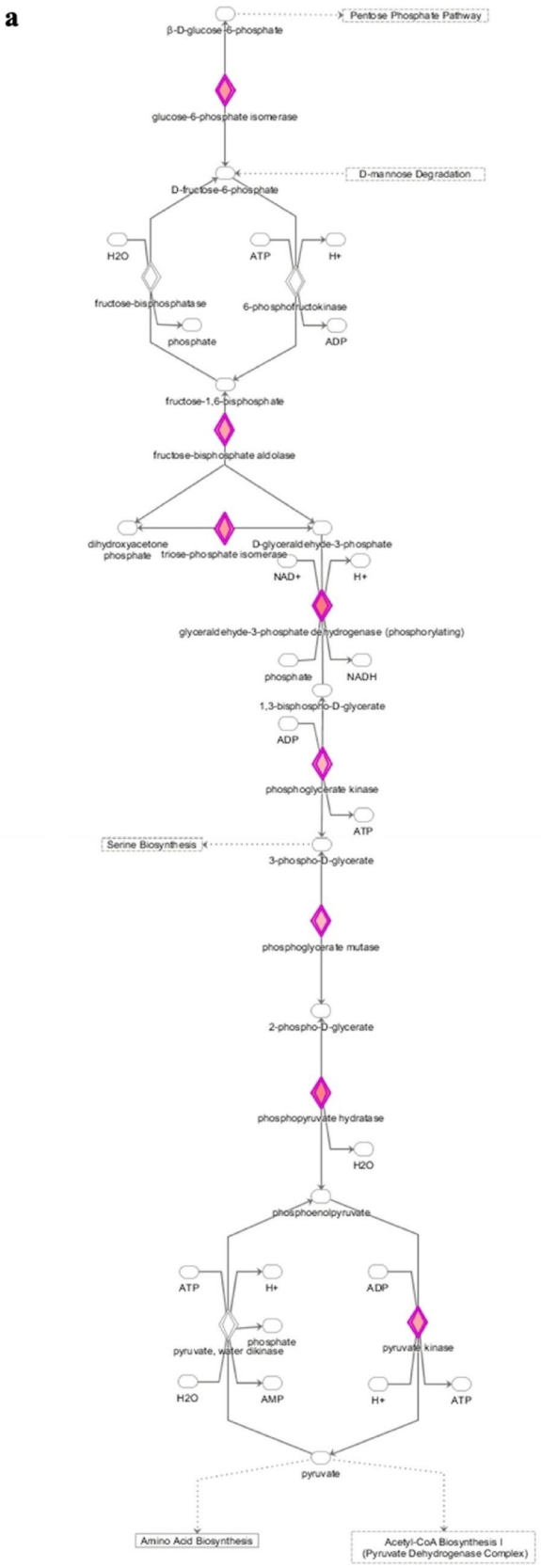

Fig. 4 De-induction from hypobaric hypoxia to sea level up-regulates carbohydrate metabolism. **a** Expanded view of IPA mined glycolysis pathway with overlaid modulated proteins (pink outlined) identified in saliva proteome, **b** expanded view of IPA mined gluconeogenesis pathway with overlaid modulated proteins (pink outlined) identified in saliva proteome

of headache after descend to sea level from high altitude (Savourey et al. 1996; Boning et al. 1997; Hansen and Sander 2003; Risso et al. 2007; He et al. 2013; Zhao et al. 2016; Mairbaurl 2018; Gonzalez et al. 2005). A single omics based study has been performed using plasma and suggested a panel of metabolites involved in steroid hormone biosynthesis pathway (Liu et al. 2017). The lack of omics-based studies holds necessity of studying molecular signatures and pathways involved in high-altitude de-acclimatization using proteomics-based approach by taking saliva as a diagnostic sample.

In this article, we have discussed two important observations pertaining to clinical use. First, significant changes in the redox system in saliva samples suggesting its role as an indicator of de-acclimatization. Many researchers have reported an increase in oxidative stress and antioxidant enzymes (as an adaptive response) in response to hypobaric hypoxia in various organ systems (Jefferson et al. 2004; Magalhaes, et al. 1985; Maiti et al. 2006; Devi et al. 2007; Rauchova et al. 2005). Also, Gustavo González et al. reported modulations in oxidative damage in membrane lipids after re-oxygenation conditions (Gonzalez et al. 2005). In our study, oxidative stress parameters, ROS was found to be highest in HAD30 group and decreased levels were observed at DI 30 group as compared to HAD30. As ROS was not the only marker for oxidative stress, lipid peroxides levels were also estimated and found to be normalized in every group. Antioxidants such as catalase and GSH showed no significant difference in the levels of activity at HAD30 group as compared to N and at DI 30 group as compared to HAD30.

Second, in response to de-acclimatization, carbohydrate metabolism was found to be activated when compared with high-altitude exposure group and sea level normoxic controls. We observed perturbations in pathways such as glycolysis and gluconeogenesis. Earlier reports also suggested modifications in enzymes of carbohydrate metabolism in response to hypobaric hypoxic exposure and re-oxygenation studies (Funasaka et al. 2005; Goto et al. 2015; Hara and Watanabe 2020; Sharma et al. 2013). An important protein having twofold increase in de-acclimatization group as compared to high-altitude induction group, alpha-enolase, is a well-known hypoxia tolerance marker and a

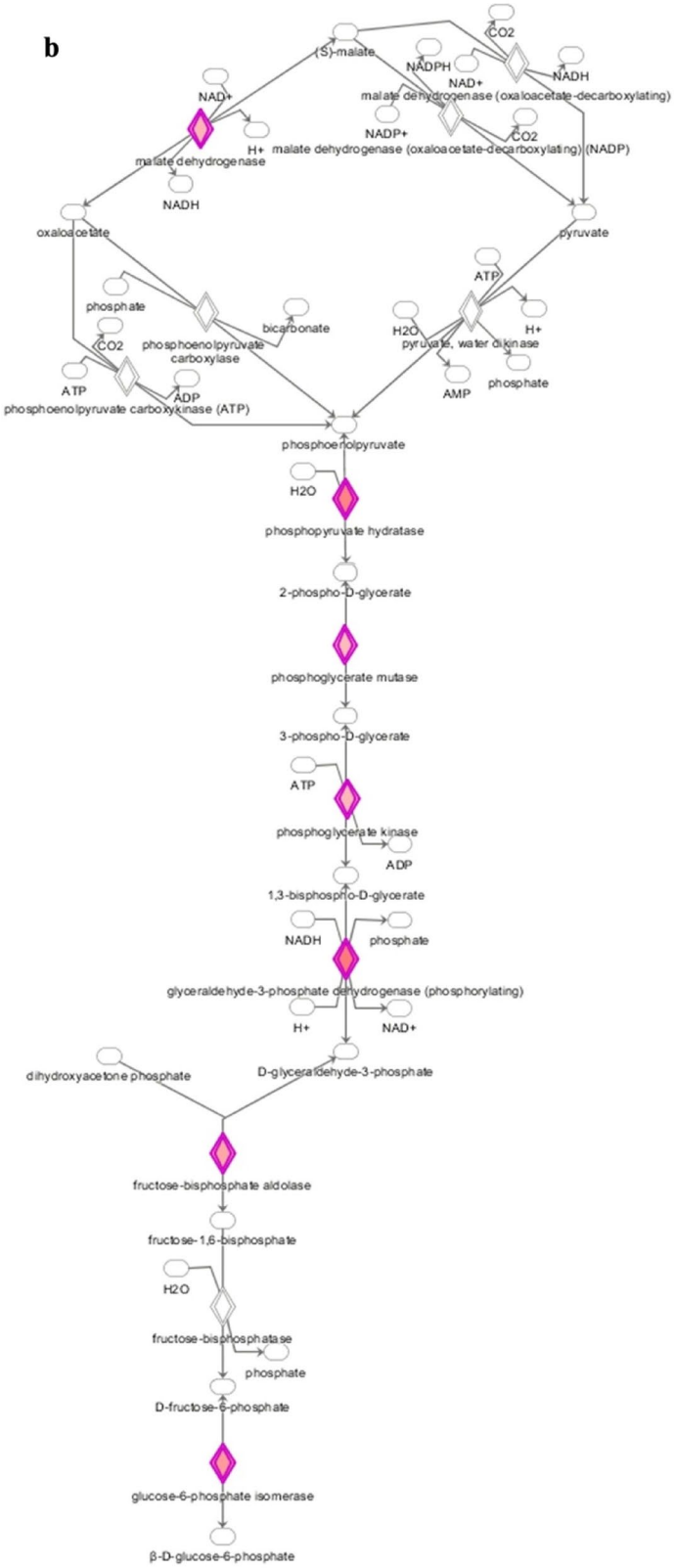

Fig. 4 (continued)

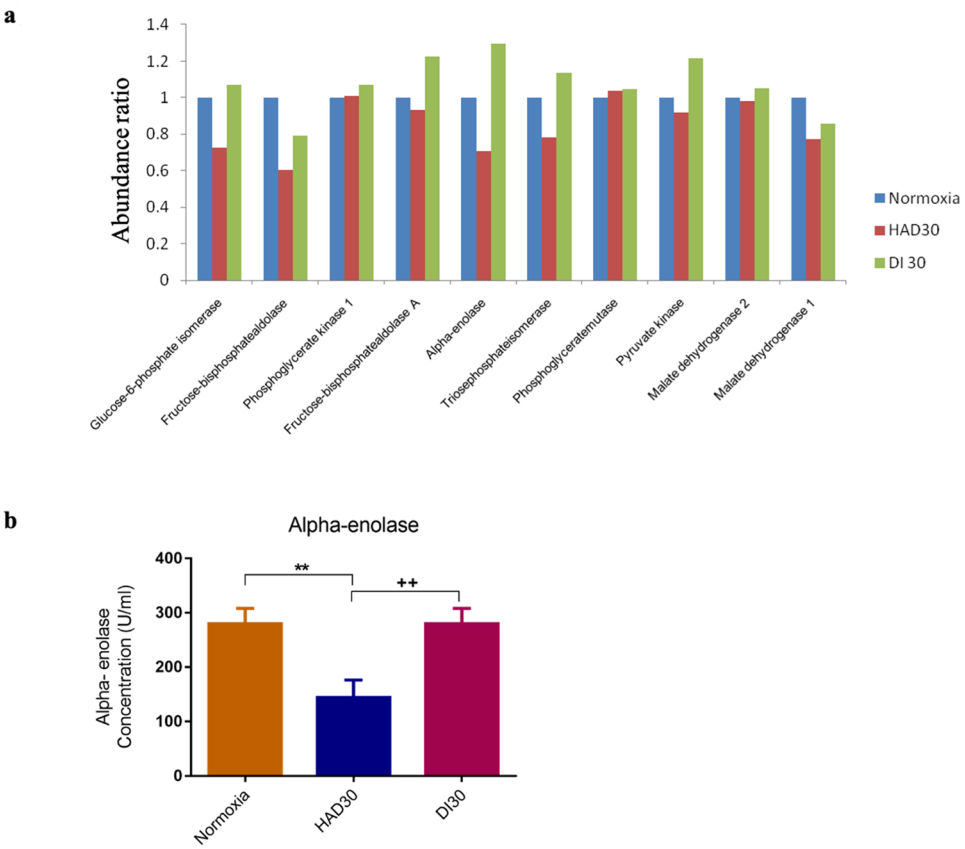

Fig. 5 Putative proteins involved in glycolysis and gluconeogenesis. **a** Abundance ratio values of proteins involved in the pathways (p value < 0.05). **b** Alpha-enolase levels were validated in saliva samples of N, HAD30 and DI 30 groups using ELISA. The levels decreased in HAD30 from N followed by an increase in DI 30 group. Results are expressed as Mean concentration ± SD. Mean was calculated from three separate experimental replicates (**represents p value < 0.05 with respect to N and $^{++}$ represents p value < 0.05 with respect to HAD30, sample size = 24)

multifunctional enzyme, known to be involved in various processes such as growth control, allergic responses, as well as glycolysis other than inflammatory hypoxic tolerance. It has several interacting partners such as Pyruvate Kinase, Phosphoglycerate Kinase and Glyceraldehyde 3-phosphate Dehydrogenase. Earlier, also it has been observed in various hypoxic studies and well established with hypoxia induced physiological changes (Kim et al. 2006; Semenza et al. 1996), suggesting its role as potential protein marker (Mikuriya et al. 2007; Xu et al. 2005). A study by Cunxiu Fan et al. suggested that neuron-specific enolase (NSE) significantly decreased during high-altitude exposure but significantly increased after descent to sea-level (Fan et al. 2016). This protein was already shown to be expressive in our preliminary hypobaric hypoxia exposure studies (Jain et al. 2020; Jain et al. 2018).

In addition to carbohydrate metabolism pathways, LXR/RXR activation and acute phase response signalling pathways were also found to be modulated. These two pathways have already been discussed in our previous study on salivary proteome in response to hypobaric hypoxia (Jain et al. 2020).

Another redox protein, thioredoxin, Trx known to prevent the elevation of superoxide radicals and hydrogen peroxide by blocking the xanthine oxidase (XOD) enzyme which converts hypoxanthine to xanthine (Araneda and Tuesta 2012). Earlier in-vivo studies of recombinant Trx is also known to prevent ischemia–reperfusion injury in cardiomyocytes probably by reducing ROS when administrated to rat and rabbit as a model (Heusch 2020). In our study, we have validated human Trx protein in the saliva samples and observed that Trx is down-regulated in HAD30 group and drastically up-regulated in DI30 group. Hence, it can be further suggested that after descent form high altitude, there is an occurrence of signal transduction cascade due to Trx that facilitate proper gaseous exchange; and prevents oedema formation in the blood capillaries and lipid peroxidation in humans to avoid further complications.

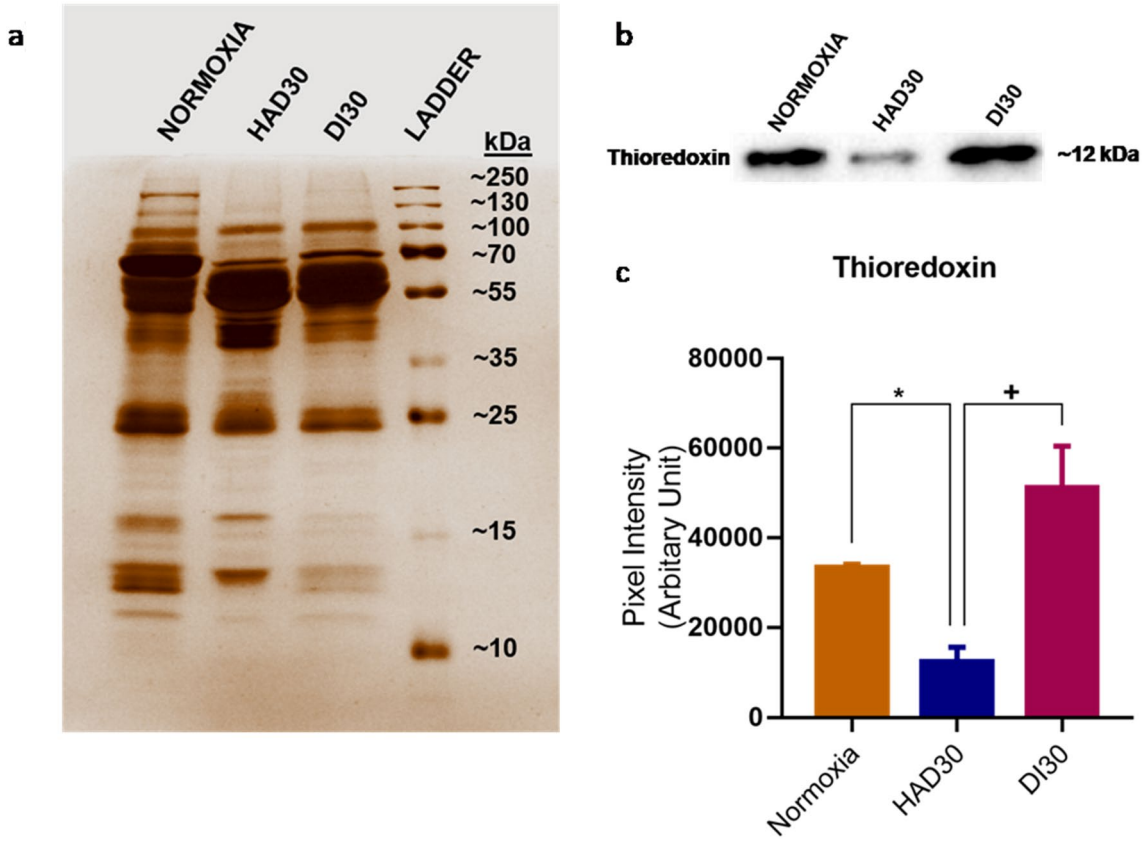

Fig. 6 Modifications in levels of Thioredoxin **a** Silver-stained SDS PAGE gel of the equally loaded saliva samples collected from the normoxic controls and individuals from experimental group. **b** Thioredoxin levels were validated in saliva samples of N, HAD30 and DI 30 groups using immunoblotting. **c** Densitometry analysis suggested that the thioredoxin levels decreased in HAD30 from N followed by an increase in DI 30 group. Results are expressed as Mean concentration ± SD. Mean was calculated from three separate experimental replicates (*represents p value < 0.1 with respect to N and $^{+}$ represents p value < 0.1 with respect to HAD30, sample size = 24)

Conclusion

In conclusion, this study provided the initial advancement in understanding high-altitude de-acclimatization-mediated events through salivary proteome. Carbohydrate metabolism was a significantly activated pathway in response to de-acclimatization to high altitude. Key proteins modulated in this pathway were Glucose-6-phosphate isomerase, Fructose-bisphosphate aldolase, Phosphoglycerate kinase 1, Fructose-bisphosphate aldolase A, Glyceraldehyde-3-phosphate dehydrogenase, Alpha-enolase, Triosephosphate isomerase, Phosphoglycerate mutase, Pyruvate kinase, Malate dehydrogenase 2 and Malate dehydrogenase 1. Alpha-enolase levels were up-regulated (nearly two-folds) in DI 30 group as compared to HAD30, thereby making it a putative biomarker for activated carbohydrate metabolism in response to de-acclimatization to high altitude.

Study limitations

This is an initial study that needs to be further validated over large population in order to obtain a better understanding of the events mediated in de-acclimatization to high altitude. In spite of the author's best efforts, these limitations do remain.

Supplementary Information The online version contains supplementary material available at https://doi.org/10.1007/s42485-023-00109-5.

Acknowledgements We would like to acknowledge Dr. Bhuvnesh Kumar, former Director, DIPAS, DRDO and Dr. Rajeev Varshney, Director, DIPAS, DRDO for extending logistical support and necessary permissions to recruit suitable volunteers for this study.

Author contributions Conceived and designed the experiments by YA and KB. Experiments were performed by SJ. Representative figures were designed by SJ. Manuscript was written by SJ. Manuscript was critically evaluated by YA and KB. Sections related to Thioredoxin were performed and written by SM.

Funding This work was supported by grants (DIP-263) from Defence Research and Development Organization (DRDO), Ministry of Defence, Government of India. Shikha Jain was recipient of Senior Research Fellowship from University Grants Commission (UGC). Swaraj Mohanty is recipient of Senior Research Fellowship from DRDO, Ministry of Defence, Government of India.

Data statement All queries for raw data files may be directed towards the corresponding authors, Kalpana Bhargava, Sc 'F' (kalpanab@hemrl.drdo.in; kalpanab2006@gmail.com) and Yasmin Ahmad, Sc 'E' (yasminchem@gmail.com).

Declarations

Conflict of interest The authors declare that they have no known competing financial interests or personal relationships that could have appeared to influence the work reported in this paper. We confirm that the manuscript has been read and approved by all named authors. We further confirm that the order of authors listed in the manuscript has been approved by all of us. We understand that the Corresponding Author is the sole contact for the Editorial process. He/she is responsible for communicating with the other authors about progress, submissions of revisions and final approval of proofs.

References

Ahmad Y et al (2013) An insight into the changes in human plasma proteome on adaptation to hypobaric hypoxia. PLoS ONE 8(7):e67548

Ahmad Y et al (2014) Proteomic identification of novel differentiation plasma protein markers in hypobaric hypoxia-induced rat model. PLoS ONE 9(5):e98027

Ahmad Y et al (2015) The proteome of hypobaric induced hypoxic lung: insights from temporal proteomic profiling for biomarker discovery. Sci Rep 5:10681

Araneda OF, Tuesta M (2012) Lung oxidative damage by hypoxia. Oxid Med Cell Longev 2012:856918

Boning D et al (1997) After-effects of a high altitude expedition on blood. Int J Sports Med 18(3):179–185

de Jong EP et al (2010) Quantitative proteomics reveals myosin and actin as promising saliva biomarkers for distinguishing premalignant and malignant oral lesions. PLoS ONE 5(6):e11148

Denny P et al (2008) The proteomes of human parotid and submandibular/sublingual gland salivas collected as the ductal secretions. J Proteome Res 7(5):1994–2006

Deshwal R, Iqbal M, Basnet S (2012) Nifedipine for the treatment of high altitude pulmonary edema. Wilderness Environ Med 23(1):7–10

Devi SA et al (2007) Intermittent hypobaric hypoxia-induced oxidative stress in rat erythrocytes: protective effects of vitamin E, vitamin C, and carnitine. Cell Biochem Funct 25(2):221–231

Fan C et al (2016) Reversible brain abnormalities in people without signs of mountain sickness during high-altitude exposure. Sci Rep 6:33596

Funasaka T et al (2005) Regulation of phosphoglucose isomerase/autocrine motility factor expression by hypoxia. FASEB J 19(11):1422–1430

Gallo C et al (2016) Potential salivary proteomic markers of oral squamous cell carcinoma. Cancer Genomics Proteomics 13(1):55–61

Giusti L et al (2007) Proteome analysis of whole saliva: a new tool for rheumatic diseases—the example of Sjogren's syndrome. Proteomics 7(10):1634–1643

Gonzalez G et al (2005) Red cell membrane lipid changes at 3500 m and on return to sea level. High Alt Med Biol 6(4):320–326

Goto K et al (2015) Augmented carbohydrate oxidation under moderate hypobaric hypoxia equivalent to simulated altitude of 2500 m. Tohoku J Exp Med 236(3):163–168

Grassl N et al (2016) Ultra-deep and quantitative saliva proteome reveals dynamics of the oral microbiome. Genome Med 8(1):44

Grocott M, Montgomery H, Vercueil A (2007) High-altitude physiology and pathophysiology: implications and relevance for intensive care medicine. Crit Care 11(1):203

Hansen J, Sander M (2003) Sympathetic neural overactivity in healthy humans after prolonged exposure to hypobaric hypoxia. J Physiol 546(Pt 3):921–929

Hara Y, Watanabe N (2020) Changes in expression of genes related to glucose metabolism in liver and skeletal muscle of rats exposed to acute hypoxia. Heliyon 6(7):e04334

Hartmann G et al (2000) High altitude increases circulating interleukin-6, interleukin-1 receptor antagonist and C-reactive protein. Cytokine 12(3):246–252

He B et al (2013) Analysis of high-altitude de-acclimatization syndrome after exposure to high altitudes: a cluster-randomized controlled trial. PLoS ONE 8(5):e62072

Heusch G (2020) Myocardial ischaemia-reperfusion injury and cardioprotection in perspective. Nat Rev Cardiol 17(12):773–789

Hodinka RL, Nagashunmugam T, Malamud D (1998) Detection of human immunodeficiency virus antibodies in oral fluids. Clin Diagn Lab Immunol 5(4):419–426

Hu S, Loo JA, Wong DT (2006) Human body fluid proteome analysis. Proteomics 6(23):6326–6353

Hu S et al (2007) Salivary proteomic and genomic biomarkers for primary Sjogren's syndrome. Arthritis Rheum 56(11):3588–3600

Hu S et al (2008) Salivary proteomics for oral cancer biomarker discovery. Clin Cancer Res 14(19):6246–6252

Jain S, Ahmad Y, Bhargava K (2018) Salivary proteome patterns of individuals exposed to High Altitude. Arch Oral Biol 96:104–112

Jain S et al (2020) Saliva panel of protein candidates: a comprehensive study for assessing high altitude acclimatization. Nitric Oxide 95:1–11

Jefferson JA et al (2004) Increased oxidative stress following acute and chronic high altitude exposure. High Alt Med Biol 5(1):61–69

Jessie K, Hashim OH, Rahim ZHA (2008) Protein precipitation method for salivary proteins and rehydration buffer for two-dimensional electrophoresis. Biotechnology 7(4):686–693

Jia Z et al (2020) Impacts of the plateau environment on the gut microbiota and blood clinical indexes in Han and Tibetan individuals. mSystems 5(1):e00660-19

Kim JW et al (2006) HIF-1-mediated expression of pyruvate dehydrogenase kinase: a metabolic switch required for cellular adaptation to hypoxia. Cell Metab 3(3):177–185

Levett DZ et al (2011) The role of nitrogen oxides in human adaptation to hypoxia. Sci Rep 1:109

Liu C et al (2017) Activated corticosterone synthetic pathway is involved in poor responses to re-oxygenation after prolonged hypoxia. Int J Clin Exp Pathol 10(8):8414–8423

Loo JA et al (2010) Comparative human salivary and plasma proteomes. J Dent Res 89(10):1016–1023

Luks AM et al (2017) Changes in acute pulmonary vascular responsiveness to hypoxia during a progressive ascent to high altitude (5300 m). Exp Physiol 102(6):711–724

Magalhaes J et al (2005) Acute and severe hypobaric hypoxia increases oxidative stress and impairs mitochondrial function in mouse skeletal muscle. J Appl Physiol 99(4):1247–1253

Mairbaurl H (2018) Neocytolysis: how to get rid of the extra erythrocytes formed by stress erythropoiesis upon descent from high altitude. Front Physiol 9:345

Maiti P et al (2006) Hypobaric hypoxia induces oxidative stress in rat brain. Neurochem Int 49(8):709–716

Mikuriya K et al (2007) Expression of glycolytic enzymes is increased in pancreatic cancerous tissues as evidenced by proteomic profiling by two-dimensional electrophoresis and liquid chromatography-mass spectrometry/mass spectrometry. Int J Oncol 30(4):849–855

Peluso G et al (2007) Proteomic study of salivary peptides and proteins in patients with Sjogren's syndrome before and after pilocarpine treatment. Arthritis Rheum 56(7):2216–2222

Rauchova H, Vokurkova M, Koudelova J (2005) Developmental changes of erythrocyte catalase activity in rats exposed to acute hypoxia. Physiol Res 54(5):527–532

Risso A et al (2007) Red blood cell senescence and neocytolysis in humans after high altitude acclimatization. Blood Cells Mol Dis 38(2):83–92

Savourey G et al (1996) Pre-adaptation, adaptation and de-adaptation to high altitude in humans: cardio-ventilatory and haematological changes. Eur J Appl Physiol Occup Physiol 73(6):529–535

Semenza GL et al (1996) Hypoxia response elements in the aldolase A, enolase 1, and lactate dehydrogenase A gene promoters contain essential binding sites for hypoxia-inducible factor 1. J Biol Chem 271(51):32529–32537

Sharma NK, Sethy NK, Bhargava K (2013) Comparative proteome analysis reveals differential regulation of glycolytic and antioxidant enzymes in cortex and hippocampus exposed to short-term hypobaric hypoxia. J Proteomics 79:277–298

Siervo M et al (2014) Effects of prolonged exposure to hypobaric hypoxia on oxidative stress, inflammation and gluco-insular regulation: the not-so-sweet price for good regulation. PLoS ONE 9(4):e94915

Streckfus CF et al (2008) Breast cancer related proteins are present in saliva and are modulated secondary to ductal carcinoma in situ of the breast. Cancer Invest 26(2):159–167

Wang H, Joseph JA (1999) Quantifying cellular oxidative stress by dichlorofluorescein assay using microplate reader. Free Radic Biol Med 27(5–6):612–616

Xiao H et al (2012) Proteomic analysis of human saliva from lung cancer patients using two-dimensional difference gel electrophoresis and mass spectrometry. Mol Cell Proteomics 11(2):M111.012112

Xu RH et al (2005) Inhibition of glycolysis in cancer cells: a novel strategy to overcome drug resistance associated with mitochondrial respiratory defect and hypoxia. Cancer Res 65(2):613–621

Yaari A et al (2006) Detection of HCV salivary antibodies by a simple and rapid test. J Virol Methods 133(1):1–5

Yan JX et al (2000) A modified silver staining protocol for visualization of proteins compatible with matrix-assisted laser desorption/ionization and electrospray ionization-mass spectrometry. Electrophoresis 21(17):3666–3672

Zhao JP et al (2016) Characteristics of EEG activity during high altitude hypoxia and lowland reoxygenation. Brain Res 1648(Pt A):243–249